

УДК: 612.82.(616-006+616-073.175):617.7-003.669-073.8
DOI: 10.24061/2413-4260.XVI.1.59.2026.20

R. Navruzov¹, Sh. Teshayev¹, G. Yusupaliyeva²,
Z. Saydullayev³

Bukhara State Medical Institute¹
(Bukhara, Republic of Uzbekistan),
Tashkent State Medical University²
(Tashkent, Republic of Uzbekistan),
Samarkand State Medical University³
(Samarkand, Republic of Uzbekistan)

MORPHOMETRIC CRITERIA FOR THE ASSESSMENT OF MASS EFFECT IN INTRACRANIAL SPACE-OCCUPYING LESIONS BASED ON MAGNETIC RESONANCE IMAGING DATA

Summary.

Intracranial space-occupying lesions are associated with the development of mass effect, manifesting as displacement of midline structures, cortical deformation, compression of the ventricular system, and disturbance of cerebrospinal fluid dynamics. Despite the widespread use of magnetic resonance imaging (MRI), quantitative morphometric criteria for the assessment of mass effect severity remain insufficiently standardised.

Study Objective. *To identify and systematise morphometric parameters enabling objective assessment of the degree of mass effect in intracranial space-occupying lesions based on MRI data.*

Materials and Methods. *A retrospective study of brain MRI in patients with intracranial space-occupying lesions was conducted. The analysis included measurement of midline shift, lesion volume, perifocal oedema volume, ventricular system dimensions and indices (including the Evans index), degree of subarachnoid space deformation, and hemispheric asymmetry. Morphometric analysis was performed using 3D T1-weighted images and automated segmentation methods. All procedures were conducted in accordance with the Declaration of Helsinki of the World Medical Association (2000 amendment). Statistical analysis was performed using SPSS version 22.0 and MedCalc. The normality of data distribution was assessed using the Shapiro–Wilk test. Between-group comparisons were performed using the Mann–Whitney U test, Student’s t-test, Pearson’s chi-squared test, and Spearman’s correlation analysis. Predictive performance was evaluated by receiver operating characteristic (ROC) analysis with calculation of the area under the curve (AUC). Statistical significance was defined at $p < 0.05$. The study was conducted at Bukhara State Medical Institute as part of the institutional research entitled «Development of Novel Approaches to Early Detection, Treatment, and Prevention of Pathological Conditions Affecting the Health of the Population of the Bukhara Region in the Post-COVID-19 Pandemic Period (2022-2026).»*

Results. *The severity of mass effect was found to correlate significantly with lesion volume and perifocal oedema volume. The most sensitive morphometric parameters were the magnitude of midline shift (> 5 mm), the degree of ventricular system compression, and hemispheric asymmetry. Combined assessment of multiple parameters enhances the objectivity of diagnosis and enables stratification of disease severity.*

Conclusion. *Quantitative MR morphometry is an informative and reproducible method for the assessment of mass effect in intracranial space-occupying lesions. Standardisation of morphometric criteria may contribute to improved accuracy of preoperative evaluation and optimisation of treatment strategy.*

Keywords: *Mass Effect; Morphometry; Brain; Space-Occupying Lesions; MRI; Neuroimaging.*

Introduction

Intracranial space-occupying lesions represent one of the most clinically significant causes of intracranial hypertension and secondary structural changes of the central nervous system. Regardless of their morphological nature – whether neoplasms, haematomas, abscesses, or cysts – these processes are accompanied by an increase in intracranial volume, the development of mass effect, and disruption of the spatial relationships among the anatomical structures of the brain [1-3]

Mass effect is characterised by displacement of midline structures, compression of the ventricular system, deformation of cortical and subcortical formations, and alteration of cerebrospinal fluid dynamics. The severity of these changes directly influences clinical symptomatology, the risk of herniation syndromes, and disease prognosis [4, 5]. In routine neuroradiology practice, the assessment of mass effect has traditionally been predominantly qualitative in nature and dependent upon the subjective experience of the reporting specialist, which reduces reproducibility and hampers the comparison of findings across centres [6-8].

Contemporary magnetic resonance imaging (MRI) offers extensive capabilities for the quantitative analysis of structural brain changes. The application of morphometric methods, including automated segmentation and three-dimensional reconstruction, enables objective quantification of midline shift, lesion volume, perifocal oedema, and ventricular system changes [9-12]. Quantitative assessment of these parameters contributes to the standardisation of diagnostic criteria and enhances the accuracy of disease monitoring [13-15].

Nevertheless, a systematic framework of morphometric criteria for the comprehensive assessment of mass effect severity remains insufficiently established in the literature. The absence of unified quantitative threshold values hampers the stratification of disease severity and the selection of optimal therapeutic strategy, including the determination of indications for urgent neurosurgical intervention [16-18].

In this context, the development of a comprehensive morphometric approach to the assessment of mass effect in intracranial space-occupying lesions based on MRI data is of considerable relevance [19-21]. Such an approach would enhance diagnostic accuracy, improve

preoperative planning, and optimise longitudinal patient monitoring, whilst providing the basis for the development of standardised algorithms for severity assessment.

Study Objective. To identify and systematise morphometric parameters enabling objective assessment of the degree of mass effect in intracranial space-occupying lesions based on MRI data.

Materials and Methods

A retrospective study of brain MRI in patients with intracranial space-occupying lesions was conducted. The analysis included measurement of midline shift, lesion volume, perifocal oedema volume, ventricular system dimensions and indices (including the Evans index), degree of subarachnoid space deformation, and hemispheric asymmetry. Morphometric analysis was performed using 3D T1-weighted images and automated segmentation methods.

All procedures were conducted in accordance with the Declaration of Helsinki of the World Medical Association (2000 amendment).

Statistical analysis was performed using SPSS version 22.0 and MedCalc. The normality of data distribution was assessed using the Shapiro–Wilk test. Between-group comparisons were performed using the Mann–Whitney U test, Student’s t-test, Pearson’s chi-squared test, and Spearman’s correlation analysis. Predictive performance was evaluated by receiver operating characteristic (ROC) analysis with calculation of the area under the curve (AUC). Statistical significance was defined at $p < 0.05$.

The study was conducted at Bukhara State Medical Institute as part of the institutional research plan entitled «Development of Novel Approaches to Early Detection, Treatment, and Prevention of Pathological Conditions Affecting the Health of the Population of the Bukhara Region in the Post-COVID-19 Pandemic Period (2022-2026).»

Results

Patients with intracranial space-occupying lesions of varying aetiology and location were enrolled in the study. Quantitative morphometric analysis enabled the identification of systematic patterns of structural brain changes and the determination of the most informative criteria for mass effect assessment.

General Characteristics of Morphometric Changes

In all cases of space-occupying processes, signs of spatial displacement of brain structures were observed, varying in degree of severity. The principal changes included:

- lateral displacement of midline structures;
- deformation of cortical gyri;
- compression of the ventricular system;
- narrowing of the subarachnoid spaces;
- alteration of the grey-to-white matter ratio in the zone of involvement.

The severity of these parameters was dependent upon lesion volume, its location, and the degree of perifocal oedema.

Midline Shift

Displacement of the septum pellucidum, third ventricle, and pineal gland was recorded in the majority of patients. Mean shift values ranged from 2 to 9 mm.

The threshold of clinical significance (> 5 mm) was exceeded in more than half of the patients.

At a displacement of $> 8-10$ mm, signs of early herniation changes were identified.

A pronounced positive correlation was demonstrated between total lesion volume and the degree of midline shift ($r = 0.62-0.74$; $p < 0.05$).

Lesions located in the temporal and parietal lobes were associated with more pronounced lateral displacement compared with frontal lobe localisation (Table 1).

Table 1

Morphometric criteria for mass effect in space-occupying lesions (MRI)

Parameter (what is measured)	Normal / minimal mass effect	Threshold values in mass effect	Clinical significance
Midline shift	0 mm	≤ 3 mm (moderate), 4-7 mm (marked), ≥ 8 mm (critical)	Displacement of the interhemispheric fissure, third ventricle, and brainstem
Displacement of vascular structures	Absent	Up to deformation	Vascular compression; risk of ischaemia
Ventricular size and shape	Normal	Partial compression → marked compression / dilatation	Indicator of impaired cerebrospinal fluid drainage / intracranial pressure elevation
Lesion volume (cm ³)	0	< 30 cm ³ , 30-50 cm ³ , > 50 cm ³	Assessed by planimetry on T1/T2/FLAIR sequences
White matter oedema (perifocal)	Absent	Moderate → marked	Assessed by the width of the hyperintensity zone on T2/FLAIR sequences
Transtentorial herniation	Absent	Present / absent	Critical indicator of displacement
Subfalcine herniation	Absent	Present / absent	Assessed by displacement of the interhemispheric fissure
Compression of basal cisterns	Absent	Partial / complete	Indicative of elevated intracranial pressure
Internal hydrocephalus	Absent	Present / absent	Ventricular dilatation secondary to impaired drainage

Lesion Volume and Perifocal Oedema

Lesion volumes varied across a wide range. Morphometric analysis enabled their classification into

small (< 20 cm³), intermediate (20-50 cm³), and large (> 50 cm³) categories. Perifocal oedema substantially increased the total lesion volume, by a mean of 35-65%.

Characteristic features:

The tumour tissue demonstrates heterogeneous hypointensity relative to the unaffected white matter, with central zones of marked hypointensity corresponding to areas of necrosis. The lesion margins are ill-defined and infiltrative in character, extending in the craniocaudal direction along the white matter (Figure 1 Signs of mass involvement are present:

local deformation of cortical structures and partial effacement of the adjacent sulci The longitudinal extent of infiltration is more conspicuous on sagittal sections, underscoring the tendency of glioblastoma to spread along the white matter.

Coronal sections demonstrate a large, structurally heterogeneous space-occupying lesion with pronounced perifocal vasogenic oedema.

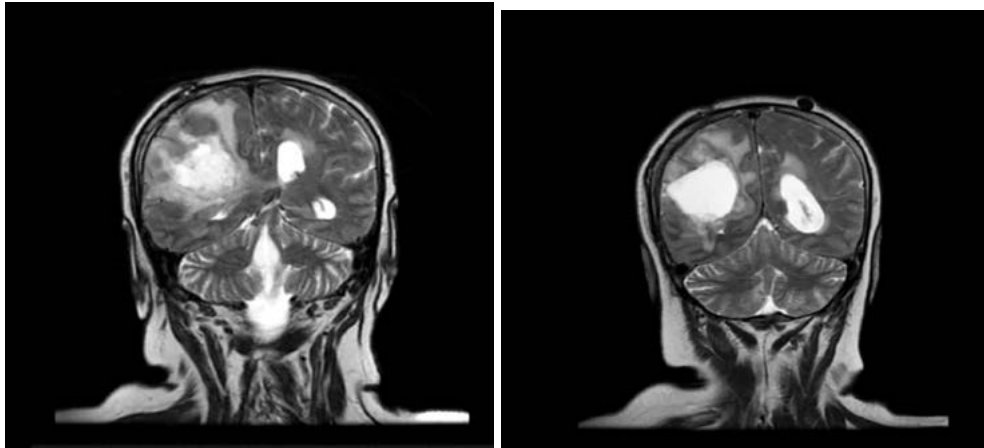


Figure 1. A heterogeneous, hyperintense space-occupying lesion in the right parieto-temporal region with marked perifocal oedema (glioblastoma; T2-weighted MRI, coronal sections).

On T2-weighted imaging, glioblastoma is typically represented as a heterogeneous hyperintense space-occupying lesion. Characteristic features include heterogeneously increased signal intensity within the tumour due to a combination of tumour tissue, areas of micro- and macroscopic necrosis, cystic changes, and perifocal oedema; ill-defined infiltrative margins reflecting tumour spread along white matter tracts; and pronounced

vasogenic oedema extending over considerable distances from the primary lesion node, resulting in increased volume of the affected hemisphere. Mass effect manifests as local sulcal effacement, deformation of adjacent structures, and possible midline shift. In T2-weighted sequences, glioblastoma thus presents as a large, bright, structurally heterogeneous focus with zonal organisation (Figure. 2).

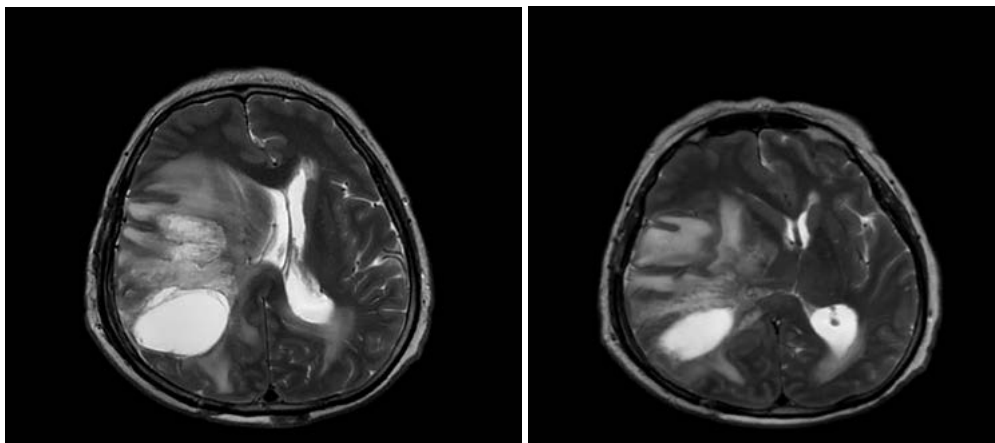


Figure 2. A heterogeneous, hyperintense space-occupying lesion in the right parieto-temporal region with marked perifocal oedema (glioblastoma; T2-weighted MRI, axial projection).

The following findings were established:

- a total volume (lesion plus oedema) exceeding 40 cm³ was associated with a significant increase in the risk of pronounced mass effect;

- at deep locations, even intermediate-volume lesions produced marked ventricular deformation.

Accordingly, total lesion volume proved to be a more informative parameter than tumour volume assessed in isolation.

Assessment of ventricular system changes in intracranial space-occupying lesions revealed several patterns:

compression of the ipsilateral lateral ventricle was the most frequently observed finding; contralateral dilatation secondary to septal displacement was also commonly identified; and obstructive hydrocephalus developed in cases involving the cerebrospinal fluid pathways. The Evans index increased proportionally to the severity of cerebrospinal fluid dynamic disturbances, with values exceeding 0.30 more frequently associated with clinical signs of intracranial hypertension. The degree of ventricular compression correlated with the degree of lateral shift ($r = 0.58$; $p < 0.05$). Morphometric analysis also demonstrated pronounced hemispheric asymmetry

and cortical changes, including increased volume of the affected hemisphere due to oedema, gyral flattening and reduced sulcal depth, local cortical thickening in the zone of perifocal changes (pseudothickening), and, in cases of chronic progression, secondary contralateral cortical thinning. The interhemispheric asymmetry index increased significantly in the presence of pronounced mass effect ($p < 0.05$).

Комплексная количественная модель оценки масс-эффекта. На основании совокупного анализа предложена градация степени масс-эффекта:

Mass effect denotes the degree of pressure exerted by a focal lesion – whether haemorrhage, neoplasm, oedema, or other process – upon the brain parenchyma. Its clinical significance is assessed on the basis of midline shift, ventricular

system changes, and total lesion volume. In moderate mass effect, midline displacement is limited (≤ 3 mm), ventricular morphology is essentially preserved, lesion volume is less than 30 cm^3 , and the clinical condition is generally stable. In marked mass effect, displacement reaches 4-7 mm, partial ventricular compression is present, lesion volume ranges from 30 to 50 cm^3 , and clinical decompensation with neurological deterioration is possible. In critical mass effect, displacement is ≥ 8 mm, the ventricular system is severely compressed or dilated, lesion volume exceeds 50 cm^3 , and the risk of cerebral herniation is high, necessitating urgent intervention. In general, greater midline shift and total lesion volume are associated with a higher risk of intracranial hypertension and life-threatening complications (Table 2).

Table 2.

Grading of mass effect severity

Grade of mass effect	Midline shift	Ventricular changes	Total lesion volume	Clinical significance
I (moderate)	≤ 3 mm	Absent / minimal	$< 30 \text{ cm}^3$	Stable condition
II (marked)	4-7 mm	Partial compression	$30\text{-}50 \text{ cm}^3$	Decompensation possible
III (critical)	≥ 8 mm	Marked compression / dilatation	$> 50 \text{ cm}^3$	High risk of herniation

A composite index incorporating lesion volume, magnitude of midline shift, and degree of ventricular changes demonstrated superior diagnostic sensitivity compared with the isolated assessment of any single parameter.

Quantitative MR morphometry proved highly informative in the objective assessment of mass effect in intracranial space-occupying lesions. The most significant morphometric parameters were total lesion volume, midline shift, degree of ventricular compression and dilatation, and the interhemispheric asymmetry index. The severity of mass effect was significantly associated with the level of intracranial hypertension and the degree of focal neurological deficit, with impaired consciousness observed at midline shifts exceeding 8 mm. Patients with grade III mass effect more frequently required urgent neurosurgical intervention. Combined analysis of these parameters enhances the accuracy of severity stratification and may be incorporated into algorithms for preoperative assessment and longitudinal patient monitoring.

Discussion

The findings confirm that mass effect in intracranial space-occupying lesions constitutes a complex of structural changes encompassing both the direct mechanical impact of the pathological focus and secondary disturbances of cerebrospinal fluid dynamics, venous drainage, and regional perfusion [22, 23]. Quantitative MR morphometry enabled objective assessment of the degree of these changes and identification of the most informative evaluation parameters, which is consistent with current trends in neuroimaging directed towards standardisation and improvement of result reproducibility [24].

Midline shift emerged as one of the key parameters, demonstrating a consistent correlation with total lesion volume (lesion volume plus perifocal oedema) and clinical severity [25]. However, isolated assessment of midline shift does not always permit adequate estimation of the risk of decompensation, particularly in cases of deep lesion localisation, where marked compression may coexist with relatively moderate displacement [26].

Assessment of ventricular system changes is of particular importance. Compression of the ipsilateral lateral ventricle and contralateral dilatation reflect redistribution of intracranial volumes and impairment of cerebrospinal fluid circulation. The inclusion of ventricular parameters in standardised assessment protocols is warranted, as disturbance of cerebrospinal fluid circulation may accelerate the progression of intracranial hypertension and clinical deterioration [27].

The role of perifocal oedema merits separate consideration. The data obtained demonstrated that total lesion volume more accurately predicts the degree of herniation changes compared with tumour volume assessed in isolation. This is of particular relevance in neoplastic processes, where oedema may substantially exceed the dimensions of the tumour itself and determine the clinical presentation [28, 29].

Analysis of interhemispheric asymmetry and cortical changes indicated that prolonged mass effect may lead to secondary atrophy of contralateral structures. Dynamic quantitative assessment of such changes using automated image analysis and machine learning methods enhances prognostic accuracy and may be applied in surgical planning [30].

The superiority of the comprehensive approach was demonstrated upon comparison of isolated and combined parameters, as the integration of multiple morphometric parameters increases diagnostic sensitivity and enables more accurate stratification of mass effect severity.

In addition to the quantitative assessment of mass effect, contemporary surgical approaches to complications associated with intracranial space-occupying lesions or secondary pathological processes warrant consideration. Modern minimally invasive techniques, including laparoscopic intervention for recurrent hernias, have demonstrated high efficacy and a reduction in postoperative complications. These approaches underscore the necessity of comprehensive structural analysis and preoperative planning accounting for individual patient anatomy, which may be of particular relevance in combined pathological conditions and complex focal topography within the brain.

The limitations of the study include its retrospective design, potential heterogeneity in the morphological

structure of the lesions, and the influence of MRI technical parameters on segmentation accuracy. Prospective studies employing unified protocols and incorporating machine learning algorithms and statistical methods for reproducibility assessment are warranted.

The results thus confirm that quantitative MR morphometry is a reliable instrument for the objective assessment of mass effect and holds considerable potential for the standardisation of neuroradiological diagnosis, optimisation of preoperative planning, and improvement of clinical outcomes.

Conclusions

The present study has demonstrated that quantitative MR morphometry enables objective assessment of mass effect severity in intracranial space-occupying lesions. The following key morphometric criteria reflecting the degree of brain structure displacement and compression were identified:

- displacement of midline structures (in particular, the septum pellucidum and third ventricle);
- ventricular system changes (compression, dilatation, elevation of the Evans index);
- total lesion volume (lesion volume plus perifocal oedema);
- hemispheric asymmetry and cortical deformation.

Total lesion volume was shown to reflect mass effect severity more accurately than tumour volume assessed in isolation. Combined evaluation of multiple morphometric parameters enhances diagnostic accuracy and enables stratification of patients by severity grade (moderate, marked, and critical), which is of practical significance for preoperative planning and longitudinal monitoring. Brain MR morphometry thus represents a promising instrument for the standardisation of mass effect assessment and may be implemented in clinical practice to improve diagnosis and inform treatment strategy.

Prospects for further research. Future research perspectives are associated with the expansion of the patient sample and the conduct of multicentre studies to enhance the statistical validity of the findings. The development of

a standardised morphometric protocol for the assessment of mass effect in intracranial space-occupying lesions using multiple MRI sequences is considered warranted.

The investigation of associations between quantitative morphometric parameters and clinical manifestations, the degree of neurological deficit, and disease prognosis represents a relevant avenue of inquiry. The implementation of automated image analysis methods based on artificial intelligence technologies to improve the accuracy and reproducibility of measurements is also considered promising.

Further study is required to correlate morphometric criteria with surgical treatment outcomes and longitudinal patient monitoring in the postoperative period.

Author Contributions: R. Navruzov – study concept and design, MRI data analysis, manuscript writing; Sh. Teshayev – clinical data collection, statistical data processing, manuscript editing; G. Yusupaliyeva – interpretation of study results, methodological consultation, critical revision of manuscript content; Z. Saydullayev – study organisation, coordination of the author team, final approval of the manuscript version for publication.

All authors have read the final version of the manuscript and given their consent for publication.

Conflict of Interest. The authors declare no conflict of interest in relation to the preparation and publication of this article.

Funding. The study was conducted without external funding. No financial support was received from governmental, commercial, or non-profit organisations.

Acknowledgements. The authors express their sincere gratitude to the staff of the clinics and departments of Bukhara State Medical Institute and Tashkent State Medical University for their valuable contributions to the organisation of the study, assistance with the collection and processing of clinical and MRI material, and methodological guidance throughout the research process.

References:

1. Tellez D, Litjens G, Bándi P, Bulten W, Bokhorst JM, Ciompi F, et al. Quantifying the effects of data augmentation and stain color normalization in convolutional neural networks for computational pathology. *Med Image Anal.* 2019;58:101544. DOI: <http://doi.org/10.1016/j.media.2019.101544> PMID: 31466046.
2. Efron B, Tibshirani RJ. *An Introduction to the Bootstrap.* Boca Raton (FL): CRC Press; 1994. 456 p. DOI: <http://doi.org/10.1201/9780429246593>
3. Iizuka O, Kanavati F, Kato K, Rambeau M, Arihiro K, Tsuneki M. Deep Learning Models for Histopathological Classification of Gastric and Colonic Epithelial Tumours. *Sci Rep.* 2020;10(1):1504. DOI: <http://doi.org/10.1038/s41598-020-58467-9> PMID: 32001752; PMCID: PMC6992793.
4. Adel Fahmideh M, Scheurer ME. Pediatric Brain Tumors: Descriptive Epidemiology, Risk Factors, and Future Directions. *Cancer Epidemiol Biomarkers Prev.* 2021;30(5):813-21. DOI: <http://doi.org/10.1158/1055-9965.EPI-20-1443> PMID: 33653816.
5. Cole BL. Neuropathology of Pediatric Brain Tumors: A Concise Review. *Neurosurgery.* 2022;90(1):7-15. DOI: <http://doi.org/10.1093/neuros/nyab182> PMID: 34114043.
6. Niazi MKK, Parwani AV, Gurcan MN. Digital pathology and artificial intelligence. *Lancet Oncol.* 2019;20(5):e253-61. DOI: [http://doi.org/10.1016/S1470-2045\(19\)30154-8](http://doi.org/10.1016/S1470-2045(19)30154-8) PMID: 31044723; PMCID: PMC8711251.
7. Echle A, Rindtorff NT, Brinker TJ, Luedde T, Pearson AT, Kather JN. Deep learning in cancer pathology: a new generation of clinical biomarkers. *Br J Cancer.* 2021;124(4):686-96. DOI: <http://doi.org/10.1038/s41416-020-01122-x> PMID: 33204028; PMCID: PMC7884739.
8. Davlatov S, Navruzov R, Sanoyeva M, Xudoykulov D, Gaziev K. Case of laparoscopic treatment recurrent obturator hernia. In: *Global Summit on Life Sciences and Bio-Innovation: From Agriculture to Biomedicine (GLSBIA 2024).* BIO Web Conf. [Internet]. 2024[cited 2025 Dec 29];121:04003. 7p. Available from: https://www.bio-conferences.org/articles/bioconf/abs/2024/40/bioconf_glsbia2024_04003/bioconf_glsbia2024_04003.html DOI: <http://doi.org/10.1051/bioconf/202412104003>
9. Davlatov S, Rakhmanov K, Usarov S, Yuldoshev F, Xudaynazarov U, Tuxtayev J. Inguinal hernia: modern aspects of etiopathogenesis and treatment. *International Journal of Pharmaceutical Research.* 2020;Suppl 2:338. DOI: <http://doi.org/10.31838/ijpr/2020.SP2.338>
10. Wang X, Yang S, Zhang J, Wang M, Zhang J, Yang W, et al. Transformer-based unsupervised contrastive learning for histopathological image classification. *Med Image Anal.* 2022;81:102559. DOI: <http://doi.org/10.1016/j.media.2022.102559> PMID: 35952419.

11. Bengs M, Bockmayr M, Schüller U, Schlaefel A. Medulloblastoma tumor classification using deep transfer learning with multi-scale Efficient Nets [Internet]. In: Digital and Computational Pathology 2021 Feb 15-20; United States. SPIE; 2021[cited 2026 Jan 17];116030D. 6p. Available from: <https://www.spiedigitallibrary.org/conference-proceedings-of-spie/11603/2580717/Medulloblastoma-tumor-classification-using-deep-transfer-learning-with-multi-scale/10.1117/12.2580717.full> DOI: <http://doi.org/10.1117/12.2580717>
12. Osborn AG, Hedlund GL, Salzman KL. Osborn's Brain: Imaging, Pathology, and Anatomy. 2nd ed. Philadelphia (PA): Elsevier; 2017. 1300 p.
13. Navruzov R, Ismoilov J, Bahadir Khanov M, Almatova U, Djuraev J, Mikhiddinov A, et al. Analysis and prediction of different stages of brain tumor from MRI using AI models. Health Leadership and Quality of Life. 2024;(3):12. DOI: <http://doi.org/10.56294/hl2024.188>
14. Ezzidi A, Fakhir B, Aboufalah A, Asmouki H, Soummani A. Prenatal Diagnosis and Optimal Management of Occipital Encephalocele: A Report of Four Cases and Literature Review. Sch Int J Obstet Gynec. 2025;8(5):186-93. DOI: <https://doi.org/10.36348/sijog.2025.v08i05.008>
15. Zhou J, Enewold L, Stojadinovic A, Clifton GT, Potter JF, Peoples GE, et al. Incidence rates of exocrine and endocrine pancreatic cancers in the United States. Cancer Causes Control. 2010;21(6):853-61. DOI: <http://doi.org/10.1007/s10552-010-9512-y> PMID: 20182788.
16. Raymond E, Dahan L, Raoul JL, Bang YJ, Borbath I, Lombard-Bohas C, et al. Sunitinib malate for the treatment of pancreatic neuroendocrine tumors. N Engl J Med. 2011;364(6):501-13. DOI: <http://doi.org/10.1056/NEJMoa1003825> PMID: 21306237.
17. Timmerman R, Paulus R, Galvin J, Michalski J, Straube W, Bradley J, et al. Stereotactic body radiation therapy for inoperable early stage lung cancer. JAMA. 2010;303(11):1070-6. DOI: <http://doi.org/10.1001/jama.2010.261> PMID: 20233825; PMCID: PMC2907644.
18. Jemal A, Fedewa SA. Lung Cancer Screening With Low-Dose Computed Tomography in the United States-2010 to 2015. JAMA Oncol. 2017;3(9):1278-81. DOI: <http://doi.org/10.1001/jamaoncol.2016.6416> PMID: 28152136; PMCID: PMC5824282.
19. Tait SD, Ren Y, Horton CC, Oshima SM, Thomas SM, Wright S, et al. Characterizing participants in the North Carolina Breast and Cervical Cancer Control Program: A retrospective review of 90,000 women. Cancer. 2021;127(14):2515-24. DOI: <http://doi.org/10.1002/cncr.33473> PMID: 33826758; PMCID: PMC8320193.
20. Darrow DP. Focused Ultrasound for Neuromodulation. Neurotherapeutics. 2019;16(1):88-99. DOI: <http://doi.org/10.1007/s13311-018-00691-3> PMID: 30488340; PMCID: PMC6361056.
21. Chaudhuri A, Pragma Ghosh NS. Role of Conventional MRI with MR Spectroscopy in Evaluation of Intracranial Space Occupying Lesions. European Journal of Cardiovascular Medicine. 2025;15(8):884-92. DOI: <http://doi.org/10.61336/ejcm/25-08-161>
22. Panda AK, Sadhashivam S, Arora RK, Mittal RS, Saxena S, Nandolia K. Magnetic Resonance Imaging-Based Morphometric Analysis of the Tentorial Notch in a North Indian Population: A Descriptive Anatomical Study. Indian Journal of Neurosurgery. 2025. DOI: <http://doi.org/10.1055/s-0045-1811656>
23. Fiala G, Plass M, Harb R, Regitnig P, Skok K, Al Zoughbi W, et al. From slides to AI-ready maps: Standardized multi-layer tissue maps as metadata for artificial intelligence in digital pathology. Artificial Intelligence in Medicine. 2026;174:103368. DOI: <https://doi.org/10.1016/j.artmed.2026.103368>
24. Sansby E, Driver CJ, Borland K, Schofield I, Michou J. The sedative effect of intravenous butorphanol in dogs with intracranial space occupying lesions or indicators of intracranial hypertension. Veterinary Anaesthesia and Analgesia. 2025;52(1):61-7. DOI: <https://doi.org/10.1016/j.vaa.2024.11.006>
25. Das D, Mahanta LB, Ahmed S, Baishya BK, Haque I. Study on Contribution of Biological Interpretable and Computer-Aided Features Towards the Classification of Childhood Medulloblastoma Cells. J Med Syst. 2018;42(8):151. DOI: <http://doi.org/10.1007/s10916-018-1008-4> PMID: 29974336.
26. Das D, Mahanta LB, Ahmed S, Baishya BK. Classification of childhood medulloblastoma into WHO-defined multiple subtypes based on textural analysis. J Microsc. 2020;279(1):26-38. DOI: <http://doi.org/10.1111/jmi.12893> PMID: 32271463.
27. Phan HTH, Kumar A, Kim J, Feng D. Transfer learning of a convolutional neural network for HEP-2 cell image classification [Internet]. In: 2016 IEEE 13th International Symposium on Biomedical Imaging (ISBI); 2016 Apr 13-16; Prague. Prague: IEEE; 2016[cited 2026 Feb 7]. p.1208-11. Available from: <http://ieeexplore.ieee.org/document/7493483/>. DOI: <http://doi.org/10.1109/ISBI.2016.7493483>
28. Gertych A, Swiderska-Chadaj Z, Ma Z, Ing N, Markiewicz T, Cierniak S, et al. Convolutional neural networks can accurately distinguish four histologic growth patterns of lung adenocarcinoma in digital slides. Sci Rep. 2019;9(1):1483. DOI: <http://doi.org/10.1038/s41598-018-37638-9> PMID: 30728398; PMCID: PMC6365499.
29. Narayanan BN, Krishnaraja V, Ali R. Convolutional neural network for classification of histopathology images for breast cancer detection [Internet]. In: NAECON 2019 - IEEE National Aerospace and Electronics Conference; 2019 Jul 15-19; Dayton. Dayton: IEEE; 2019[cited 2026 Feb 8]. p. 291-5. Available from: <https://ieeexplore.ieee.org/xpl/mostRecentIssue.jsp?punumber=9035665> DOI: <http://doi.org/10.1109/NAECON46414.2019>
30. Ehteshami Bejnordi B, Veta M, Johannes van Diest P, van Ginneken B, Karsssemeijer N, Litjens G, et al. Diagnostic Assessment of Deep Learning Algorithms for Detection of Lymph Node Metastases in Women With Breast Cancer. JAMA. 2017;318(22):2199-210. DOI: <http://doi.org/10.1001/jama.2017.14585> PMID: 29234806; PMCID: PMC5820737.
31. Yu CY, Chung MC, Chen YJ, Wang HW, Zhou JX, Chen SL, Chen KT, Shih TT. Analysis of Upper Airway Morphology Using Four-Dimensional Dynamic MRI With Active Deep Learning-Based Automatic Segmentation. Journal of Magnetic Resonance Imaging. 2026.14p. DOI: <https://doi.org/10.1002/jmri.70237>

МОРФОМЕТРИЧНІ КРИТЕРІЇ ОЦІНКИ МАСОВОГО ЕФЕКТУ ПРИ ВНУТРІШНЬОЧЕРЕПНИХ УТВОРЕННЯХ, ЩО ЗАЙМАЮТЬ ПРОСТІР, НА ОСНОВІ ДАНИХ МАГНІТНО-РЕЗОНАНСНОЇ ТОМОГРАФІЇ

Р. Наврузов¹, Ш. Тешаєв¹, Г. Юсуплієва², З. Сайдұлласєв³

Бухарський державний медичний інститут¹

(м. Бухара, Республіка Узбекистан),

Ташкентський державний медичний університет²

(м. Ташкент, Республіка Узбекистан),

Самаркандський державний медичний університет³

(м. Самарканд, Республіка Узбекистан)

Резюме.

Внутрішньочерепні об'ємні утворення супроводжуються розвитком масивного ефекту, що проявляється зміщенням структур середньої лінії, деформацією кори головного мозку, компресією шлуночкової системи та порушенням динаміки спинномозкової рідини. Незважаючи на широке застосування магнітно-резонансної томографії (МРТ), кількісні морфометричні критерії для оцінки тяжкості масивного ефекту залишаються недостатньо стандартизованими.

Мета дослідження. Визначити та систематизувати морфометричні параметри, що дозволяють об'єктивно оцінити ступінь масивного ефекту при внутрішньочерепних об'ємних утвореннях на основі даних МРТ.

Матеріали та методи. Проведено ретроспективне дослідження МРТ головного мозку у пацієнтів з внутрішньочерепними об'ємними ураженнями. Аналіз включав вимірювання зміщення середньої лінії, об'єму ураження, об'єму перифокального набряку, розмірів та індексів шлуночкової системи (включно з індексом Еванса), ступеня деформації субарахноїдального простору та асиметрії півкуль. Морфометричний аналіз проводили з використанням 3D-зображень з T1-зважуванням та методів автоматизованої сегментації. Усі процедури проводилися відповідно до Гельсінської декларації Всесвітньої медичної асоціації (поправка 2000 року). Статистичний аналіз проводили за допомогою SPSS версії 22.0 та MedCalc. Нормальність розподілу даних оцінювали за допомогою тесту Шапіро–Вілка. Міжгрупові порівняння проводили за допомогою U-критерію Манна–Уїтні, t-критерію Стюдента, критерію хі-квадрат Пірсона та кореляційного аналізу Спірмена. Прогностичну ефективність оцінювали за допомогою аналізу ROC-кривої з розрахунком площі під кривою (AUC). Статистичну значущість визначали при $p < 0,05$. Дослідження проводилося в Бухарському державному медичному інституті в рамках інституційного дослідження під назвою «Розробка нових підходів до раннього виявлення, лікування та профілактики патологічних станів, що впливають на здоров'я населення Бухарської області в післяпандемічний період COVID-19 (2022-2026 рр.)».

Результати. Встановлено, що тяжкість масивного ефекту суттєво корелює з об'ємом вогнища та об'ємом перифокального набряку. Найчутливішими морфометричними параметрами були величина зміщення середньої лінії (> 5 мм), ступінь компресії шлуночкової системи та асиметрія півкуль. Комплексна оцінка декількох параметрів підвищує об'єктивність діагнозу та дозволяє стратифікувати тяжкість захворювання.

Висновок. Кількісна МР-морфометрія є інформативним та відтворюваним методом оцінки масивного ефекту при внутрішньочерепних об'ємних ураженнях. Стандартизація морфометричних критеріїв може сприяти підвищенню точності передопераційної оцінки та оптимізації стратегії лікування.

Ключові слова: масивний ефект; морфометрія; мозок; об'ємні ураження; МРТ; нейровізуалізація.

Contact information:

Rustam Navruzov – Associate Professor of the Department of Nuclear Medicine and Medical Radiology of the Bukhara State Medical Institute named after Abu Ali ibn Sino. Bukhara, Uzbekistan
e-mail: rustam.navruzov.9191@gmail.com
ORCID ID: <https://orcid.org/0000-0002-8848-0795>
Scopus Author ID: <https://www.scopus.com/authid/detail.uri?authorId=59243575200>

Shukhrat Teshayev – DSc, Professor of the Department Anatomy and Clinical Anatomy, Rector of the Bukhara State Medical Institute named after Abu Ali ibn Sino. Bukhara, Uzbekistan.
E-mail: teshayev@bsmi.uz
ORCID: <https://orcid.org/0009-0002-1996-4275>
Scopus Author ID: <https://www.scopus.com/authid/detail.uri?authorId=56695400100>

Gulnora Yusupaliyeva – DSc, Professor, Head of the Department of Medical Radiology No. 2. Tashkent State Medical University
e-mail: yusupaliyeva1972@gmail.com
ORCID: <https://orcid.org/0000-0002-0768-6936>
Scopus Author ID: <https://www.scopus.com/authid/detail.uri?authorId=57193343431>

Zayniddin Saydullayev – PhD, Associate Professor, Department of General Surgery, Samarkand State Medical University, Samarkand, Uzbekistan.
ORCID ID: <https://orcid.org/0000-0003-1941-8506>
e-mail: saydullayevzayniddin8@gmail.com
Scopus Author ID: <https://www.scopus.com/authid/detail.uri?authorId=57219197241>

Контактна інформація:

Наврузов Рустам Рашидович – PhD, доцент кафедри ядерної медицини та медичної радіології Бухарського державного медичного інституту імені Абу Алі ібн Сіно (м. Бухара, Узбекистан)
e-mail: rustam.navruzov.9191@gmail.com
ORCID ID: <https://orcid.org/0000-0002-8848-0795>
Scopus Author ID: <https://www.scopus.com/authid/detail.uri?authorId=59243575200>

Тешаєв Шухрат Жумасвич – д. мед. н., професор кафедри анатомії та клінічної анатомії, ректор Бухарського державного медичного інституту імені Абу Алі ібн Сіно (м. Бухара, Узбекистан).
e-mail: teshayev@bsmi.uz
ORCID: <https://orcid.org/0009-0002-1996-4275>
Scopus Author ID: <https://www.scopus.com/authid/detail.uri?authorId=56695400100>

Юсупалієва Гулнора Акмалівна – д. мед. н., професор, завідувач кафедри медичної радіології №2 Ташкентського державного медичного університету (м. Ташкент, Узбекистан)
e-mail: yusupaliyeva1972@gmail.com
ORCID: <https://orcid.org/0000-0002-0768-6936>
Scopus Author ID: <https://www.scopus.com/authid/detail.uri?authorId=57193343431>

Сайдудласв Зайнідін Яхшибоєвич – кандидат медичних наук (PhD), доцент кафедри загальної хірургії Самаркандського державного медичного університету (м. Самарканд, Узбекистан)
e-mail: saydullayevzayniddin8@gmail.com
ORCID ID: <https://orcid.org/0000-0003-1941-8506>
Scopus Author ID: <https://www.scopus.com/authid/detail.uri?authorId=57219197241>

Received by the editorial office: 13 January 2026.

Approved for publication: 23 February 2026.

Published: 27 March 2026.

